Impact Factor:

ISRA (India)	= **4.971**	**SIS** (USA)	= **0.912**	**ICV** (Poland)	= **6.630**
ISI (Dubai, UAE)	= **0.829**	**РИНЦ** (Russia)	= **0.126**	**PIF** (India)	= **1.940**
GIF (Australia)	= **0.564**	**ESJI** (KZ)	= **8.716**	**IBI** (India)	= **4.260**
JIF	= **1.500**	**SJIF** (Morocco)	= **5.667**	**OAJI** (USA)	= **0.350**

SOI: 1.1/TAS DOI: 10.15863/TAS

International Scientific Journal

Theoretical & Applied Science

p-ISSN: 2308-4944 (print) **e-ISSN:** 2409-0085 (online)

Year: 2020 **Issue:** 01 **Volume:** 81

Published: 30.01.2020 **http://T-Science.org**

QR – Issue **QR – Article**

Bekzod Ortikov
Samarkand State University
Researcher

Nurshod Kadirov
Samarkand State University
Undergraduate of Mechanical and Mathematical Faculty

Ablakul Abdirashidov
Samarkand State University
Corresponding member of International Academy,
Doctor of Physical and Mathematical Sciences,
Professor to department of theoretical and applied mechanics,
abdira@mail.ru

MODELING THE SAFE MOVEMENT OF HYDRAULIC MANIPULATORS DURING THEIR DESIGN

***Abstract**: In this paper, the following tasks were solved to determine the characteristics of the manipulator: in the kinematic case, the operating point of the manipulator was expressed by the trajectory of the parts, their elongation, contraction and deflection angle; when the trajectory of the operating point of the manipulator is set in a kinematic position, the relationship between the elongation, compression and the angle of rotation of the parts is determined; the differential equation of motion of the manipulator is constructed; the reaction forces generated in the support of the manipulator in static conditions are determined; typical tasks were solved for the design of working mechanisms and of mechanisms the manipulator; the results were demonstrated by animation using the Maple program.*

***Key words**: manipulator, static, kinematic and dynamic states, trajectory of motion, differential equation of motion, reaction forces.*

***Language**: English*

***Citation**:* Ortikov, B., Kadirov, N., & Abdirashidov, A. (2020). Modeling the safe movement of hydraulic manipulators during their design. *ISJ Theoretical & Applied Science, 01 (81),* 485-492.

***Soi**:* http://s-o-i.org/1.1/TAS-01-81-87 ***Doi**:* crossref https://dx.doi.org/10.15863/TAS.2020.01.81.87

***Scopus ASCC**: 2206.*

Introduction

Widespread use mechanisms of manipulator (or hydromanipulator) in modern automated industries, transportation, loading, loading, mining, and other industries is a necessity today. Because it is desirable to use perfect projects to achieve efficient and high-quality production in the industry. To do this, we need to manage advanced mechanisms using modern computers [1-6]. The issues addressed in this paper and their solutions will help to revisit some of these problems in line with the needs of the time and find the best solution.

Formulation of the problem. To study the safe behavior of mechanisms in manipulator in plane and space from a kinematic and dynamic point of view and make some recommendations for its practical application. In order to determine the kinematic and dynamic characteristics of the manipulators, solve the following tasks: a) In the kinematic state, the manipulator's working point is represented by the elongation, contraction, and angle of movement of the parts; b) Determine the relation between the elongation, contraction, and the angle of deviation of parts of the manipulator's working point when given a trajectory of motion; c) Determine and solve the differential equation of the manipulative motion in a dynamic state (Fig. 1) [2,4,5].

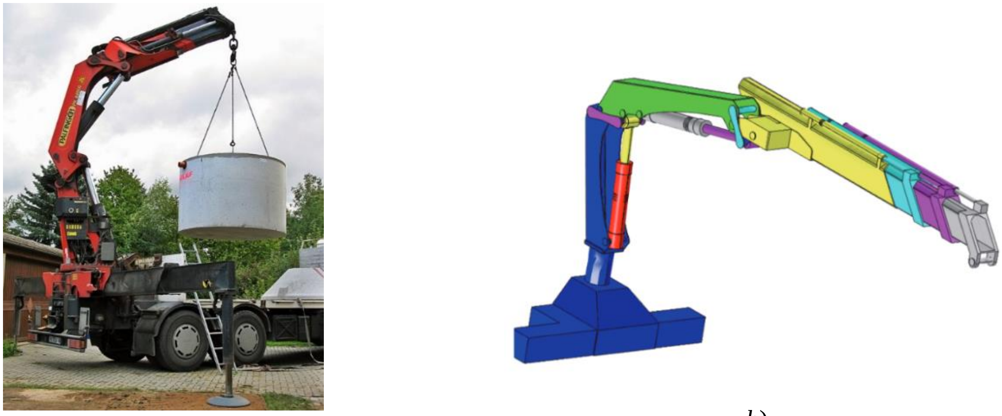

a) *b*)

Fig. 1. The object of research: a) hydromanipulator facility; b) hydromanipulator scheme.

I. Studying the law of plane motion of the manipulator working point from a kinematic and dynamic point of view.

Schematic diagram of the arrangement of hydromanipulator mechanism parts is illustrated in Fig. 2. The manipulator consists of 6 parts: *AC*, *MF*, and *EC* pistons, *OG*, *GD*, and *AD* variable. These parts are fastened to the hinge at points *M*, *G*, *F*, *E*, *D*, *C*, *K*, *A*. The operating point of the manipulator *A* is pressed into $\vec{Q}$, and it moves under the influence of the $\vec{F}_1, \vec{F}_2$ and $\vec{F}_3$ forces on the piston.

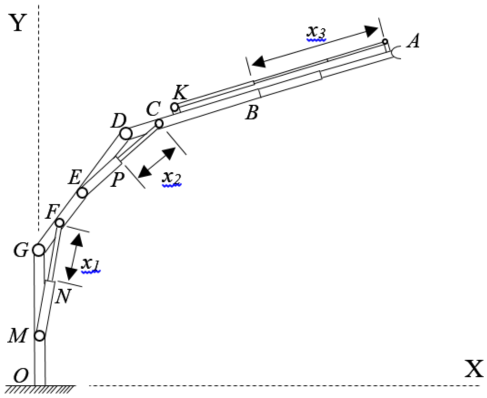

Fig. 2. Schematic arrangement of the details of the mechanism of the hydraulic manipulator on the plane.

Given:

- *dimensions of parts:*

$OG = 2;\ GD = 2.6;\ DB = 2.8;$

$MN = 1;\ EP = 0.95;\ GF = 0.5;$

$GM = 1.3;\ ED = 1.3;\ DC = 0.5$ – in meters;

- mass of parts: masses of the homogeneous *OG*, *GD*, and *AD* parts m_1, m_2 and m_3, respectively; the masses of the *MF*, *EC* and *AK* pistons are not taken into account;

the movement of the pistons in the time of τ is expressed by the $x_1(t), x_2(t), x_3(t)$ functions, here

$0 \le x_1(t) \le 0.75,\ 0 \le x_2(t) \le 0.8$

$0 \le x_3(t) \le 4.4$ when $0 \le t \le \tau$.

In this case, the law of the plane motion of the operating point of the manipulator was studied in terms of kinematics and dynamics.

The solution of the problem.

1) from the point of view of the kinematics of the projection on the coordinate axes of the operating point A of the manipulator are written as follows (Fig. 3):

$$\left.\begin{aligned} x_A(t) &= GD\cdot\cos\varphi + (DB + x_3)\cdot\cos\psi, \\ y_A(t) &= GD\cdot\sin\varphi + (DB + x_3)\cdot\sin\psi + OG. \end{aligned}\right\} \Rightarrow \left.\begin{aligned} x_A(t) &= 2.6\cos\varphi + (2.8 + x_3)\cos\psi, \\ y_A(t) &= 2.6\sin\varphi + (2.8 + x_3)\sin\psi + 2. \end{aligned}\right\} \quad (1)$$

here φ, ψ - the horizontal angles of the sections *GD* and *AD*, respectively.

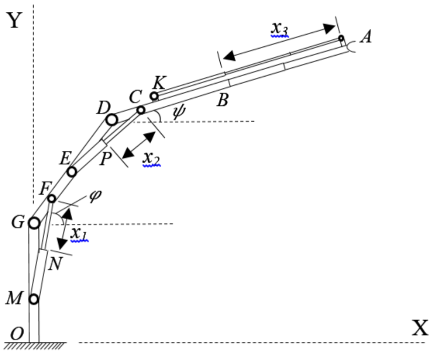

Fig. 3. Scheme for studying the law of plane motion of a manipulator from a kinematic and dynamic point of view.

Remember theorem of cosine for triangulates MGF and EDC

$$\left.\begin{aligned} (MN + x_1)^2 &= MG^2 + GF^2 - 2\cdot MG\cdot GF\cdot\cos\left(\frac{\pi}{2} + \varphi\right), \\ (EP + x_2)^2 &= ED^2 + DC^2 - 2\cdot ED\cdot DC\cdot\cos(\pi - \varphi + \psi). \end{aligned}\right\} \quad (2)$$

$$\sin\varphi = \frac{(MN + x_1)^2 - MG^2 - GF^2}{2\cdot MG\cdot GF}; \quad \cos(\varphi - \psi) = \frac{(EP + x_2)^2 - ED^2 - DC^2}{2\cdot ED\cdot DC};$$

$$\left.\begin{aligned} \varphi &= \arcsin\frac{(MN + x_1)^2 - MG^2 - GF^2}{2\cdot MG\cdot GF}, \\ \psi &= \arcsin\frac{(MN + x_1)^2 - MG^2 - GF^2}{2\cdot MG\cdot GF} + \arccos\frac{(EP + x_2)^2 - ED^2 - DC^2}{2\cdot ED\cdot DC}. \end{aligned}\right\} \quad (3)$$

$$\left.\begin{aligned} x_A(t) &= 2.6\cdot\sqrt{1 - \left(\frac{(1 + x_1)^2 - 1.94}{1.3}\right)^2} + (2.8 + x_3)\cdot\left[\sqrt{1 - \left(\frac{(1 + x_1)^2 - 1.94}{1.3}\right)^2}\cdot\right. \\ &\left.\cdot\frac{(0.95 + x_2)^2 - 1.94}{1.3} - \sqrt{1 - \left(\frac{(1 + x_1)^2 - 1.94}{1.3}\right)^2}\cdot\sqrt{1 - \left(\frac{(0.95 + x_2)^2 - 1.94}{1.3}\right)^2}\right], \\ y_A(t) &= 2 + 2.6\cdot\frac{(1 + x_1)^2 - 1.94}{1.3} + (2.8 + x_3)\cdot\left[\frac{(0.95 + x_2)^2 - 1.94}{1.3}\cdot\frac{(1 + x_1)^2 - 1.94}{1.3} + \right. \\ &\left. + \sqrt{1 - \left(\frac{(0.95 + x_2)^2 - 1.94}{1.3}\right)^2}\cdot\sqrt{1 - \left(\frac{(1 + x_1)^2 - 1.94}{1.3}\right)^2}\right]. \end{aligned}\right\} \quad (4)$$

The plane motion of point *A* at time τ is illustrated by the Maple mathematical package as follows (Fig. 4):

```
restart: with(plots): with(plottools):
OG := 2; GD := 2.6; DB := 2.8; MN := 1;
EP := .95; FG := .5;
MG:=1.3; ED:=1.3; DC:=0.5;
phi := arcsin(((MN+X1)^2-MG^2-FG^2)/(2*MG*FG));
psi := arcsin(((MN+X1)^2-MG^2-FG^2)/(2*MG*FG))+arccos(((EP+X2)^2-ED^2-DC^2)/(2*ED*DC));
XA:=GD*cos(phi)+(DB+X3)*cos(psi);
YA := GD*sin(phi)+(DB+X3)*sin(psi)+OG;
X2:=0.8; X3:=4.4; plot([XA, YA, X1 = 0 .. 5]);
```

```
X1 := .15*t; X2 := .16*t;
X3 := 4.4*sin((1/5)*Pi*t);
plot([XA, YA, t = 0 .. 5]);
ball := proc (x1, y1) local a, b, y1t;
a := plots[pointplot]([[x1, y1]], color = red, symbol = solidcircle, symbolsize = 40);
b := line([0, 0], [x1, y1], color = red);
display(a)
end proc;
animate(ball, [XA, YA], t = 0 .. 5, scaling = constrained, frames = 100);
```

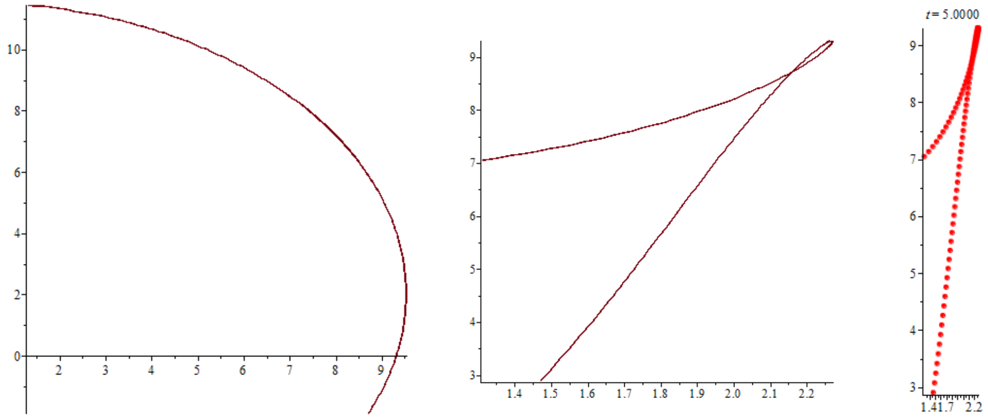

Fig. 4. Graphs showing the motion of point A on a plane in time τ.

2) The trajectory of the operating point of the manipulator is presented from the kinematic point of view in the form (Fig. 5):

$$\left.\begin{aligned} x_A(t) &= 5.8 - 0.3t, \\ y_A(t) &= 1.2 + 0.45t. \end{aligned}\right\} \tag{5}$$

Find a link between changes in parts $x_1(t), x_2(t), x_3(t)$.

The projection of the movement of the working point of the manipulator on the coordinate axes

$$\left.\begin{aligned} x_A(t) &= GD \cdot \cos\varphi + (DB + x_3) \cdot \cos\psi, \\ y_A(t) &= GD \cdot \sin\varphi + (DB + x_3) \cdot \sin\psi + OG, \end{aligned}\right\}$$

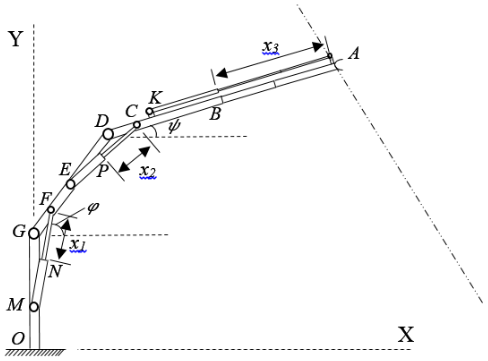

Fig. 5. Scheme for studying the law of plane motion of a manipulator from a kinematic point of view.

from here we have

$$\left.\begin{aligned} 2.6\cos\varphi + (2.8 + x_3)\cdot\cos\psi &= 5.8 - 0.3t, \\ 2.6\sin\varphi + (2.8 + x_3)\cdot\sin\psi + 2 &= 1.2 + 0.45t. \end{aligned}\right\} \tag{6}$$

Then we have

$$5.2(1.5\cos\varphi + \sin\varphi) + (2.8 + x_3)(3\cos\psi + 2\sin\psi) - 15.8 = 0$$

The plane motion of point A at time τ is illustrated by the Maple mathematical package as follows (Fig. 6):

```
restart: with(plots): with(plottools):
OG := 2; GD := 2.6; DB := 2.8; MN := 1; EP := .95; FG := .5;
 MG:=1.3; ED:=1.3; DC:=0.5;
phi := arcsin(((MN+X1)^2-MG^2-FG^2)/(2*MG*FG));
```

```
psi := arcsin(((MN+X1)^2-MG^2-FG^2)/(2*MG*FG))+arccos(((EP+X2)^2-ED^2-DC^2)/(2*ED*DC));
XA :=GD*cos(phi)+(DB+X3)*cos(psi);
YA := GD*sin(phi)+(DB+X3)*sin(psi)+OG;
X2 :=0.8; X3:=4.4; plot([XA, YA, X1 = 0 .. 5]);
X1 := .25+.1*t; X2 := .3+.1*t;
X3 := (15.8-5.2*(1.5*cos(phi)+sin(phi)))/(3*cos(psi)+2*sin(psi))-2.8;
plot([XA, YA, t = 0 .. 5]);
ball := proc (x1, y1) local a, b, y1t; a := plots[pointplot]([[x1, y1]], color = red, symbol = solidcircle, symbolsize = 40); b := line([0, 0], [x1, y1], color = red); display(a) end proc;
animate(ball, [XA, YA], t = 0 .. 5, scaling = constrained, frames = 100);
```

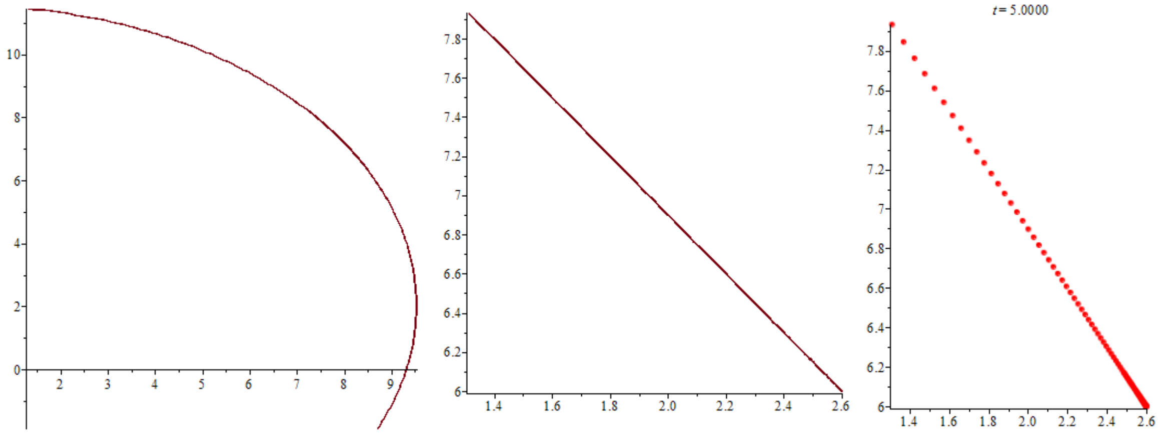

Fig 6. Graphs showing the motion of point A on a plane in time τ..

3) We use second-order Lagrangian equations to derive the differential equations of motion of the system from a dynamic point of view:

$$\frac{d}{dt}\left(\frac{\partial T}{\partial \dot{q}_i}\right) - \frac{\partial T}{\partial q_i} = Q_i\,,$$

here T – kinetic energy of the system, q_i – generalized coordinates of the system, i – degree of freedom of the system, Q_i – q_i generalized forces corresponding to generalized coordinates, and are determined by the formulas: $Q_i = \sum_{k=1}^{n} \vec{F}_k \frac{\partial \vec{r}_k}{\partial q_i}$. The degree of freedom of the manipulator mechanism is 3.

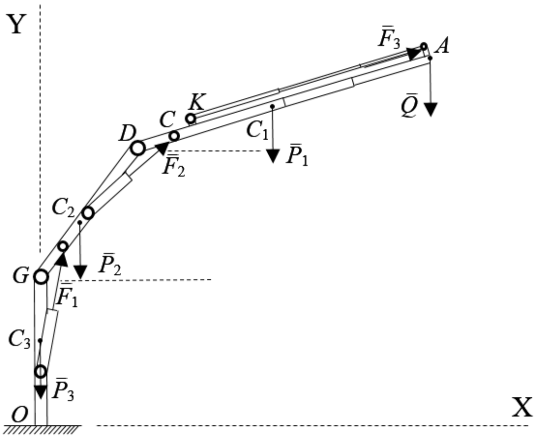

Fig. 7. Scheme for studying the law of plane motion of the operating point of the manipulator in terms of dynamics.

φ, ψ, x_3 variables are taken as the generalized coordinate of the system. $\vec{P}_1, \vec{P}_2, \vec{P}_3$ - gravity of the parts *AD*, *GD* and *OG*, respectively, C_1, C_2 - is the center of gravity of the parts AD and GD, respectively (Fig. 7).

The Lagrangian equations are written as follows:

$$\frac{d}{dt}\left(\frac{\partial T}{\partial \dot{\varphi}}\right)-\frac{\partial T}{\partial \varphi}=Q_{\varphi};\quad \frac{d}{dt}\left(\frac{\partial T}{\partial \dot{\psi}}\right)-\frac{\partial T}{\partial \psi}=Q_{\psi};\quad \frac{d}{dt}\left(\frac{\partial T}{\partial \dot{x}_3}\right)-\frac{\partial T}{\partial x_3}=Q_{x_3}. \tag{7}$$

The kinetic energy of the system is the sum of the kinetic energies of the parts *OG*, *GD*, and *AD*, respectively: $T=T_{OG}+T_{GD}+T_{AD}$, here

$$T_{OG}=0;\quad T_{GD}=\frac{m_2\cdot GD^2}{6}\dot{\varphi}^2;\quad T_{AD}=\frac{m_3}{6}\cdot AD^2\cdot\dot{\psi}^2+\frac{m_3}{2}\cdot[GD^2\cdot\dot{\varphi}^2+\frac{AD^2}{4}\cdot\dot{\psi}^2+$$
$$+\frac{\dot{x}_3^2}{4}+AD\cdot GD\cdot\dot{\varphi}\cdot\dot{\psi}\cdot\cos(\varphi-\psi)-GD\cdot\dot{\varphi}\cdot\dot{x}_3\cdot\sin(\varphi-\psi)].$$

The forces acting on the system are shown schematically in Fig. 8. Generalized coordinates φ,ψ,x_3 we determine the generalized forces $Q_\varphi, Q_\psi, Q_{x_3}$ as follows: the generalized forces $Q_\varphi, Q_\psi, Q_{x_3}$, corresponding to the generalized coordinates φ,ψ,x_3, are defined as follows:

$$Q_\varphi=[0.5F_{1y}+2.6F_{2y}+2.6F_{3y}-2.6P_1-1.3P_2-2.6Q]\cos\varphi-0.5(F_{1x}+5.2F_{2x}+5.2F_{3x})\sin\varphi;$$
$$Q_\psi=[-0.5F_{2x}-(2.8+x_3)F_{3x}]\sin\psi+[F_{2y}-(2.8+x_3)(0.5P_1+Q-F_{3y})]\cos\psi;$$
$$Q_{x_3}=F_{3x}\cos\psi+(F_{3y}-\frac{1}{2}P_1-Q)\sin\psi. \tag{8}$$

Inserting them to the Lagrange equation (7), we obtain the following system:

$$9.14m_2\ddot{\varphi}+1.3m_3\cdot\{[2\dot{x}_3\dot{\psi}+(2.8+x_3)\ddot{\psi}]\cos(\varphi-\psi)-[\ddot{x}_3+(2.8+x_3)\dot{\psi}^2]\sin(\varphi-\psi)\}=$$
$$=[0.5F_{1y}+2.6F_{2y}+2.6F_{3y}-2.6P_1-1.3P_2-2.6Q]\cos\varphi-0.5(F_{1x}+5.2F_{2x}+5.2F_{3x})\sin\varphi$$
$$1.16m_3(2.8+x_3)\dot{x}_3\dot{\psi}+0.58m_3(2.8+x_3)^2\ddot{\psi}+m_3[1.3(2.8+x_3)\ddot{\varphi}\cos(\varphi-\psi)-1.3(2.8+x_3)\cdot$$
$$\cdot\dot{\varphi}^2\sin(\varphi-\psi)]=[-0.5F_{2x}-(2.8+x_3)F_{3x}]\sin\psi+[F_{2y}-(2.8+x_3)(0.5P_1+Q-F_{3y})]\cos\psi$$
$$1.3m_3\ddot{\varphi}\sin(\varphi-\psi)-0.25m_3\ddot{x}_3+1.3m_3\dot{\varphi}^2\cos(\varphi-\psi)+0.58m_3(2.8+x_3)\dot{\psi}^2=F_{3x}\cos\psi+$$
$$+(F_{3y}-\frac{1}{2}P_1-Q)\sin\psi.$$

This system of nonlinear ordinary second-order differential equations is solved by the approximate method in the selected initial conditions. The calculation result represents the law of motion of the manipulator mechanism. If the law of change is set, the force of action of the pistons on the mechanism, then we can determine the movement of the mechanism on the plane.

II. Studying the law in space motion of the manipulator working point from a kinematic and dynamic point of view.

The scheme arrangement of parts of the manipulator mechanism is shown in Fig. 9. The parameters of the manipulator mechanism, as in the previous task, also include the spatial angle θ.

In this case, the law of motion of the operating point of the manipulator in space was studied from a kinematic point of view.

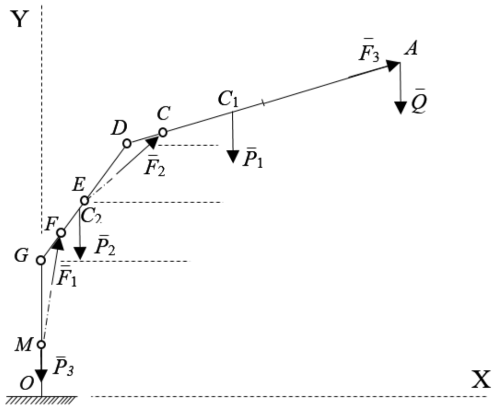
Fig. 8. Schematic representation of the forces acting on the system.

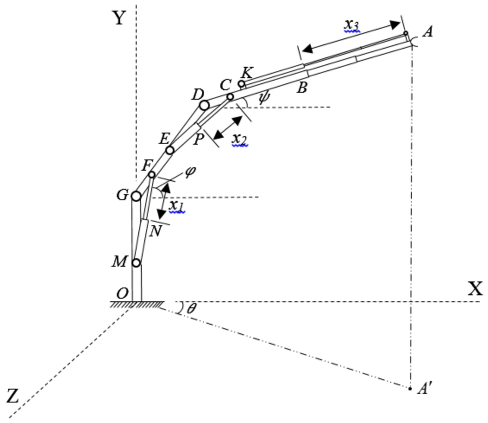
Fig. 9. Arrangement of parts of the mechanisms manipulator in space.

The solution of the problem.

1) from the point of view of the kinematics of the projection on the coordinate axes of the operating point A of the manipulator are written as follows:

$$\left.\begin{aligned} x_A(t) &= [GD\cdot\cos\varphi + (DB + x_3)\cdot\cos\psi]\cdot\cos\theta,\\ y_A(t) &= GD\cdot\sin\varphi + (DB + x_3)\cdot\sin\psi + OG,\\ z_A(t) &= [GD\cdot\cos\varphi + (DB + x_3)\cdot\cos\psi]\cdot\sin\theta. \end{aligned}\right\} \Rightarrow \left.\begin{aligned} x_A(t) &= [2.6\cdot\cos\varphi + (2.8 + x_3)\cdot\cos\psi]\cdot\cos\theta,\\ y_A(t) &= 2.6\cdot\sin\varphi + (2.8 + x_3)\cdot\sin\psi + 2,\\ z_A(t) &= [2.6\cdot\cos\varphi + (2.8 + x_3)\cdot\cos\psi]\cdot\sin\theta. \end{aligned}\right\}$$

We apply the cosine theorem to the triangles *MGF* and *EDC*, we obtain the following equalities:

$$\varphi = \arcsin\frac{(1+x_1)^2 - 1.94}{1.3}, \quad \psi = \arcsin\frac{(1+x_1)^2 - 1.94}{1.3} + \arccos\frac{(0.95+x_2)^2 - 1.94}{1.3} \tag{9}$$

The space motion of point A at time τ is illustrated by the Maple mathematical package as follows (Fig. 10):

```
restart: with(plots): with(plottools):
OG := 2; GD := 2.6; DB := 2.8; MN := 1; EP := .95; FG := .5;
 MG:=1.3; ED:=1.3; DC:=0.5;
phi := arcsin(((MN+X1)^2-MG^2-FG^2)/(2*MG*FG));
psi := arcsin(((MN+X1)^2-MG^2-FG^2)/(2*MG*FG))+arccos(((EP+X2)^2-ED^2-DC^2)/(2*ED*DC));
U := GD*cos(phi)+(DB+X3)*cos(psi);
XA:=(U)*cos(theta);
YA := GD*sin(phi)+(DB+X3)*sin(psi)+OG;
ZA := U*sin(theta);
X1 := .15*t; X2 := .8; X3 := 4.4; theta := (1/5)*Pi*t;
XX := evalf(XA); YY := evalf(YA); ZZ := evalf(ZA);
LL := proc (z, x, y) local L; L := point([z, x, y], color = blue, symbol = box, symbolsize = 10); display(L, axes = boxed, view = [-10 .. 15, -10 .. 15, -10 .. 15], orientation = [125, 65]) end proc;
animate(LL, [ZZ, XX, YY], t = 0 .. 5, scaling = constrained, trace = 50, frames = 100);
```

This animated result shows the trajectory of the spatial movement of the working point of the mechanism.

2) From a dynamic point of view, when the above problem is considered in the spatial state, the degree of freedom of the manipulator mechanism is 4. The generalized coordinates of the system are the variables $\varphi, \psi, \theta, x_3$. Lagrange equations can be used to derive differential equations of motion of a system.

The result is a system consisting of 4 simple nonlinear differential equations of the second order. This system can be solved in the selected initial conditions by some approximate method.

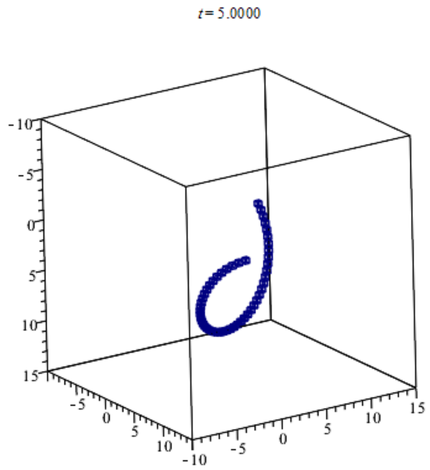

Fig. 10. The space motion of point *A* at time τ.

The result of the calculation represents the law of motion of the manipulator in space. If the law of the acting forces of the piston on the mechanism is given, then it is possible to determine the movement of the mechanism in space.

Conclusion. The mechanism of operation of the manipulator was studied on the basis of kinematic and dynamic equations: the geometric parameters of the manipulator parts were studied according to their law of motion, the differential equations of motion are derived and solved. It is advisable to design working machines, truck cranes, multi-purpose machines, hoisting devices, hydraulic manipulators, robot manipulators, crane manipulators and their mechanisms. It is possible to cooperate with existing industrial enterprises in the design of multi-purpose vehicles [1,3-12].

References:

1. Shabana, A. A. (2005). *Dynamics of Multibody system*. (p.374). Cambridge University Press.
2. Daxiyev, F. F., & Rayevskaya, L. T. (2015). Raschet obobshyennix sil lesnogo manipulyatora s chetirmya stepenyami svobodi. *Sovremenniye problemi nauki i obrazovaniya, 1-1*.
3. Kozirev, Yu. G. (2011). *Primeneniye promishlennix robotov*. (p.488). Moscow: KnoRus.
4. Lagerev, I. A., & Lagerev, A. V. (2012). *Dinamika trexzvennix gidravlicheskix kranov-manipulyatorov*. (p.196). Bryansk: Izdatelstvo BGTU.
5. Lagerev, I. A. (2016). *Modelirovaniye rabochix prosessov manipulyasionnix sistem mobilnix mnogoselevix transportno-texnologicheskix mashin i kompleksov*. (p.371). Bryansk: RIO BGU.
6. Petrenko, A. M., Zvekov, A. T. (2009). *Gruzoviye manipulyatori spesialnix transportnix sredstv*. (p.90). Moscow: MADI (GTU).
7. Rayevskaya, L. T., Shves, A. V., Daxiyev, F. F., & Ankudinov, D. T. (2013). Raschet kinematicheskix xarakteristik manipulyatora pri neizmennom ugle mejdu streloy i rukoyatyu. *Sovremenniye problemi nauki i obrazovaniya, 2*.
8. Poletaykin, V. F., & Klesnikov, P. G. (2014). *Kombinirovanniye manipulyatori lesosechnix i lesotransportnix mashin. Dinamika elementov konstruksiy*. (p.167). Krasnoyarsk: SibGTU.
9. Novoselov, V. V. (2013). Vremya peremen. Rossiyskiy rinok gidromanipulyatorov. *Stroitelnaya texnika i texnologii, 4*, pp. 98-110.
10. Sun, Y., Wan, Y., Liang, X., Huang, X., & Liu, Z. (2020). Design of a New Hydraulic Manipulator with Kinematic and Dynamic Analysis. In: Tan J. (eds) *Advances in Mechanical Design. ICMD. Mechanisms and Machine Science, 77*. Springer, Singapore.
11. Liu, Q., Ge, W. M., Wang, X. F., & Zhang, H. Y. (2018). Dynamics modeling and simulation of constrained flexible load with manipulator operation. 42(3).
12. Janne Koivumäki and Jouni Mattila. (2015). Stability-Guaranteed Force-Sensorless Contact Force/Motion Control of Heavy-Duty Hydraulic Manipulators. *IEEE Transactions on Robotics 31(4)*, pp. 918-935.